

Impact of Land Use Change on the Hydrological Regime and Flood Susceptibility in the Teusacá River Basin

Ortiz-Bernal, Laura Carolina¹, Cárdenas Bejarano, Pedro Antonio², Rivas – Trujillo, Edwin³

¹Universidad Sergio Arboleda. Bogotá. Colombia, laura.ortiz03@usa.edu.co

²Profesor Ingeniería Ambiental. Universidad Sergio Arboleda Bogotá, Colombia, pedro.cardenasb@usa.edu.co

³Profesor Titular. Facultad de Ingeniería, Universidad Distrital Francisco José de Caldas, Bogotá D.C., Colombia, erivas@udistrital.edu.co.

Abstracts

In recent years, the Teusacá River basin has experienced economic development based on agroindustrial activities, intensive grazing, and construction material exploitation. Furthermore, urban expansion and water abstraction in the San Rafael Reservoir have contributed to changes in land use and vegetation cover. These changes generate impacts that affect the hydrological balance, triggering events such as floods, droughts, and forest fires. Therefore, it is necessary to establish a relationship between land use and land cover changes and the hydrological response of the basin and, at the same time, assess the likelihood of flooding events. To this end, an integrated approach was used, utilizing models in HEC-HMS, HEC-RAS, and various maps from open data and ArcGIS to analyze the watershed's hydrological response to changes in land cover and precipitation between 2000 and 2018. The results showed that, although the curve numbers showed minimal changes between the two years, they were sufficient to generate an increase in flows of between 1 and 2 m³/s over the different return periods. The model also demonstrated that there are areas susceptible to flooding with a 5-year return period. It was evident that, in 2018, these areas showed flood patches with a depth greater than those recorded in 2000.

Keywords: Hydrological model, land use, flow, impact, susceptibility.

1. Introduction

The Teusacá River sub-basin is located in the north eastern part of the Cundinamarca Department, in the central-eastern part of the Bogotá River basin, in the Cundinamarca-Boyacá plateau. The municipalities of La Calera, Sopó, Guasca, Bogotá, Tocancipá, Choachí, Chía, and Ubaque are located within this sub-basin. Its waters flow from the Verjón and Tunjos highlands in a south-north direction until they empty into the southeastern sector of the Bogotá River [1].

The upper Teusacá River basin constitutes the main natural area near the city of Bogotá, the capital. Fundamental ecological processes emerge and take place in this area, generating resources and benefits for the population and surrounding areas. These include water

management, climate control, and air pollution control in the eastern part of the capital [2]. Both, the upper Teusacá River basin and the eastern hills have been subject to regulatory laws since the mid-20th century. These laws established the first guidelines for supervising and regulating land use and management in the basin area. Previously, people disposed of the land without regard for environmental considerations, engaging in activities such as road construction, firewood extraction, housing construction, and domestic activities. These development activities gave strength to the urbanization process, as well as to the traditional agricultural practices of the Teusacá community. In addition, the need for construction materials to meet the development needs of Bogotá led the population to participate in mining extraction activities, creating quarries for the exploitation of sand and clay [3].

Likewise, Pedraza[4]mentioned that similar phenomena occur in the middle-lower basin, since changes in the landscape and nature are observed to satisfy human needs, since in recent decades deforestation and changes in forest cover in crop and livestock production areas have increased. This allocation of use can result in a conflict of use that generates problems and negative impacts on the ecosystem, especially of the soil and water resources, since it can have various impacts on the quality and sustainability, favoring the degradation and contamination of these. The constant increase in population and accelerated urbanization makes the risk of flooding latent, putting human health and life at risk [5].

The above highlights that the Teusacá River sub-basin has provided various natural resources for human activities. Furthermore, Muñoz et al. [6], state that the Teusacá River is one of the most important tributaries of the Bogotá River, which supplies at least seven municipalities for domestic, agricultural and livestock activities, and also discharges wastewater into the river. Due to the urgency of managing resources sustainably, research is emerging that is dedicated to evaluating the behavior of water bodies considering the complex interactions between the environment and hydrology. As mentioned above, the basin has been affected by changes in land use, which directly affect its water supply [7]. Studies revealed that the different hydrological responses are linked to vegetation cover as well as to the soils [8].

For these hydrological studies, software such asHEC-HMS (Hydrologic Engineering Center-Hydrologic Modeling System) and HEC-RAS (Hydrological Engineering Center – River Analysis System)are normally used, where the first is designed to simulate the level of runoff that occurs at a specific point in a basin from a period of precipitation, while the second allowshydraulicmodeling todetermine the water level, so its main objective is to determine floodable areas. Therefore, in the present study, we intend to use both software programs with the intention of generating a more complete scenario regarding the Teusacá River, determining the outflow based on precipitation data and vegetation cover, and subsequently, evaluating whether a certain maximum flow generates flood zones around the river that could endanger the lives and infrastructure of the inhabitants of said area.

Thereare differentmethodsforcalculatingsurfacerunoffproducedbydifferentprecipitationevents; however, oneofthemostaccepted, givenitssimplicity, istheoneproposedbytheUnitedStatesSoilConservationService (USSCS). Tomeettheobjectiveofthestudy, itwasimportanttoestimatethe curve number (CN) accordingtothehydrologicalmethodoftheSoilConservationService (SCS) usedto determine

therunoffproductioncapacity after a periodofmaximumprecipitation. Prieto et al. [9]and Ibáñez [10],agreethatthismodelallowsthe cumulative surfacerunoffproducedby a stormto be obtained in a givenarea. Itisestimatedusing a combinationofland use and thesoilhydrologicalgroup, classified as A, B, C, and D, where A correspondsto a soilwith a highinfiltrationrate, whilesoilswith a lowinfiltrationrate are included in groupD [11].

2. Materials and Methods

Watershed characterization:To achieve the objectives of this study, the morphological parameters and indices of the TeusacáRiver basin were estimated (Table1) using ArcGIS software. Initially, the raster of the digital elevation model (DEM) obtained from the International Center for Tropical Agriculture (CIAT) website was downloaded, selecting the area of interest,to then identify the hydrographic network of the basin. For this purpose, the Fill tool was used to locate and fill raster sinks, removing small imperfections. The flow direction and flow accumulation tools were then used,to obtain the main hydrographic network. To determine the area and perimeter of the basin, new fields of type double were created in the attribute table, and for the basin length, the measure tool was used to draw a line from the highest point to the lowest point of the basin, equivalent to the average length of the basin, whose value was then substituted in equation 1 to obtain the average width of the study area. Knowing these parameters, the compactness, shape and elongation ratio indices were calculated using equations 2, 3 and 4 respectively.

The drainage density was calculated from the statistical analysis of the drainage network found from the Stream to feature tool, from this the information of the sum of the drainage lengths is obtained to be able to replace in equation 5. Likewise, to determine the average slope of the basin the DEM raster was used in conjunction with the slope tooland reclassify to calculate the slope percentages of the study area, and subsequently, the zonal statistics as table tool is used to use the data from the “count”column.

Table 1. Morphologica lparameter equations

Parameter	Equation	No.	Specification
Average width of the basin	$B = \frac{A}{L}$	1	Where
Compactness index	$Kc = 0.28 \frac{P}{\sqrt{A}}$	2	A: Basin area
Form index	$F = \frac{A}{L^2}$	3	L: Length of the basin
Elongation ratio	$Re = 1,128 \frac{\sqrt{A}}{L}$	4	P: Perimeter of the basin
Drain density	$Dd = \frac{A}{L}$	5	S _o : Average slope of the main channel
			L _c : Length of the main channel
			H _{mac} . Maximum height of the basin
			(msnm)

Average slope of the channel	$S_m = \frac{H_{max} - H_{min}}{L_c}$	6	H _{min} . Minimum height of the basin (msnm)
Concentration time (h)	$T_c = 0.066 \left(\frac{L_c}{\sqrt{S_o}} \right)^{0.77}$	7	I: precipitation intensity (mm/h) T: Delay period (years) t: Precipitation duration time (min)
Precipitation intensity (mm/h)	$I = \frac{k * T^m}{t^n}$	8	

The data in this column indicate the frequency with which a given slope percentage occurs. This value is multiplied by the average difference in elevations, and finally, the result is divided by the sum of the occurrences. For the average slope of the main channel, equation 6 is used, applying the minimum and maximum elevations for the area of interest. Likewise, the Kirpich formula, shown in equation 7, was used to calculate the time of concentration.

The hypsometric curve parameter was constructed by placing the values corresponding to the different heights of the basin on the ordinates and the area values that are above the corresponding heights on the abscissas, based on the total area of the basin. Again, using the DEM raster, a reclassification with equal intervals is performed. Employing the zonal statistics as table tool, a table was obtained with the maximum and minimum height values, and the area between curves, whose values are used to determine the average, cumulative, and percentage elevations. The aforementioned process is projected in Table.

Table 2. Data for the construction of the hypsometric curve.

Min Quota	Max Cota	Partial areas	Cumulative area	Area remaining on the surface	% of area	% of accumulated area	Cota Prom
2,550	2.605	88.77	88.77	375.18	23.66	100.00	2,577.5
2.605	2.681	28.92	117.69	286.41	7.71	76.34	2.643
2.681	2.754	29.43	147.12	257.48	7.84	68.63	2,717.5
2.754	2.826	38.31	185.43	228.05	10.21	60.79	2,790
2.826	2.899	34.12	219.55	189.75	9.09	50.58	2,862.5
2.899	2.963	31.68	251.23	155.63	8.44	41.48	2.931
2.963	3.026	32.19	283.41	123.95	8.58	33.04	2,994.5
3.026	3.090	27.82	311.23	91.76	7.42	24.46	3.058
3.090	3.154	18.79	330.03	63.94	5.01	17.04	3.122
3.154	3.214	14.38	344.41	45.15	3.83	12.03	3.184
3.214	3.273	12.49	356.90	30.77	3.33	8.20	3,243.5
3.273	3.337	8.70	365.60	18.28	2.32	4.87	3.305
3.337	3.410	4.50	370.10	9.58	1.20	2.55	3,373.5
3.410	3.495	3.38	373.48	5.08	0.90	1.35	3,452.5
3.495	3.640	1.70	375.18	1.70	0.45	0.45	3,567.5
		375.18			100.00		

Note: Areas (km²), Heights (msnm).

Coverage maps (2000-2018) and curve number (CN): To prepare the coverage maps, the open data of the Agustín Codazzi Institute (IGAC) were entered and the shapefiles corresponding to the area and year of interest were downloaded, subsequently the layers were processed by

clipping the layer according to the geoform of the basin, to determine the percentage of the area according to the land use classifications. The process was used to obtain the percentages for the years 2000 and 2018.

To determine the curve number, the United States Soil Conservation Service methodology was used, which required downloading the land use shapefile, soil type, and digital elevation model. Following this, a classification was made according to the hydrological group (GH) according to classification A, B, C, or D according to the methodology [12] and the survey of Geomechanical information in the Bogotá Savannah [13], which for the present investigation was based on the type of rock present. This information is accompanied by the creation of a new column that corresponds to the code equivalent to the type of land use, in line with the methodology.

Once they are classified, an intersection is made between both layers, land use and soil type, with the intersect tool. The result generates new numeric attribute fields corresponding to Pct A, Pct B, PctC, Pct D and LUValue respectively, and one more text type field named LUCode. With the help of the Field Calculator tool, it is added that LUCode is equal to the previously classified hydrological group (GH) and LUValue is equal to the Land Use code, and the other values of PctA, PctB, PctC, PctD. A value of 100 is added if they match, otherwise zero is placed. This way until all the columns are filled with PctB, PctC and PctD.

Then with the Create Table tool, the intersection shape is entered and the table name "CNLookUP" is go into, where the columns LUValue, Description, A, B, C and D are placed, and 4 additional rows are created, where the classification is added in the description: water, residential, forests and agriculture, and then the corresponding values by hydrological group. Finally, with the HEC-GeoHMS tool in the Utility option Generate CN Grid was selected, where the digital elevation model, the intersection layer, and the CNLookUP table were entered as input. The above produces the raster with the corresponding CN. To determine the average CN for each area, the raster is converted to a polygon and the area is multiplied by the curve number, divided by the total area of the watershed.

IDF curves and hyetograph: To generate the intensity-duration-frequency (IDF) curves, hydrometeorological data were collected from various stations located in San Luis 1 and 2, La Casita, San Pedro, and Parque Sopo. These data were obtained through open sources provided by the Regional Autonomous Corporation (CAR), the Institute of Hydrology, Meteorology, and Environmental Studies (IDEAM), and the Bogotá Water and Sewer Company (EEAB). From this information, the maximum daily precipitation records by month and year for each station were extracted. It is important to note that some stations presented incomplete data, so complementary information from external research was used. Furthermore, due to the difficulty in accessing more accurate data, it was decided to use precipitation records from the period between 1980 and 2014; this decision was based on data availability and reliability. To determine the calculation of curves and hyetograph, a predefined template was used, in order to obtain the coefficients necessary to complete equation 8, and also the values of the hyetographs, to be used in the HEC-HMS program, thus facilitating the process of analysis and generation of results.

Table 3. Hydrometeorological stations

Season	Code	Entity	Municipality	Latitude	Length
San Luis 1 and 2	2120040	EEAB	Bogotá	4°38' N	74°02' W
La casita	2120112	CAR	La Calera	4°38' N	74°01' W
San Pedro	2120125	IDEAM	Sopó	4°52' N	73°58' W
Parque Sopó	2120134	CAR	Sopó	4°45' N	74°01' W

Note: Hydrometeorological station information downloaded from open sources.

Modeling in HEC-HMS: Initially, the basin is delimited, for which the model basin was created using the 'Basin' Model Manager 'tool, with definition of the work area coordinates by means of 'Coordinate' System '. Subsequently, the layer containing the coordinate information was selected, in this case the digital elevation model, followed by this, the option 'Terrain Data Manager' was selected and the DEM file was uploaded, consecutively, in the options of the created window of the basin it was selected that the information to be subtracted should be extracted from " terrain 1" from the DEM file. Once done, the menu option 'GIS' - 'Preprocess Sins ', to fill empty spaces that the DEM had, then, the 'Preprocessing' tool was used Drainage ' with the intention of calculating the drainage network. Next, the 'IdentifyStreams' tool was used, with an area value smaller than the study area in order to define the micro-basins, in turn, an emission point was created to delimit the basin, corresponding to the mouth of the Teusacá River, and with the tool 'create a new break point' the point was inserted above the reference point (shape), then, with the option 'Delineate Elements' adds the prefixes for the micro-basins and sections. Following this, the information for the micro-basins is added, such as area, retention time, and curve number. The transformation method is established as SCS Unit Hydrograph and the loss method as SCS Curve Number. Subsequently, the 'Precipitation Gages' component is created, where the time interval of the hydrograph is specified, which, together with the 'Meteorological' component, Models' precipitation hyetograph values were entered, and then, with the 'Control Specification' component, the modeling time corresponding to 30 hours was indicated.

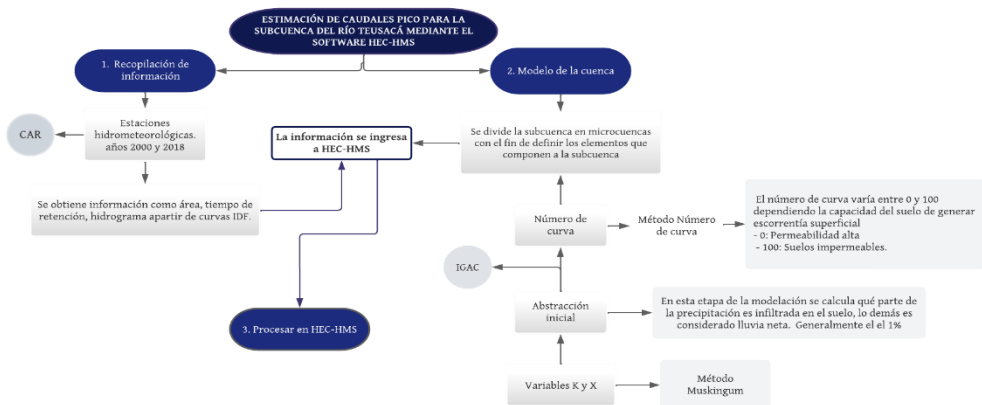


Diagram 1. Peak flow estimate for the Teusacá Riversub-basin. Hec-hms.

The Muskingum method is a flow routing technique used in hydrology to predict the propagation of a flow wave along a river or channel, which was developed by hydraulic engineer Ven Te Chow in the 1950s at the University of Iowa. This method is based on the continuity equation and the Saint-Venant wave equation to model flow behavior in a channel [14], where the program divides a channel reach into discrete segments and uses a weighted combination of kinetic storage, flux storage, and lateral flow storage to simulate flow propagation.

This parameter consists of two very important variables, the variable k and x , where k (hours) is calculated using the following equation:

$$k = \left[0.18 \cdot (\Delta x / (S_0^{0.25})) \right]^{0.76}$$

Equation 9.

Where:

Δx = Longitud del tramo

S_0 = Pendiente media

while the variable x varies between 0.0 and 0.5. It is usually set to 0.2. However, it should be noted that these parameters must meet the following condition $\Delta t > 2 \cdot k \cdot x$, if this condition is not met, the number of sub-reaches in the section must be determined, as was the case here. To do this, use the following formula:

$$\Delta t > ((2 \cdot k \cdot x)) / n \rightarrow n > (2 \cdot k \cdot x) / \Delta t$$

Equation 10.

Modeling in Hec -Ras: From the peak flows in the different return periods obtained from hec-hms, we create a new project in the hec -ras software and in the GIS-Tools menu we use the RAS -Mapper option. In the terrain section the bathymetry of the section to be studied is imported, in this case, the bathymetry was requested from the Regional Autonomous Corporation (CAR) of Cundinamarca. The bathymetry corresponds to a section of the Teusacá River located in the municipality of Sopó. Once the file is imported, with the geometry option, we add a new geometry, where the Rivers, Bank Lines options will be moved and Flow Paths, in this same order with the Start option Editing Selected Layer, the river geometry is drawn. Once this editing is complete, the river is selected and the Create Cross Section option is used with a left click. This is where the distance and length of the cross sections will be set. In this case, the length was set to 75 m and the distance between each of the cross sections was 40 m. Later, in the hec -ras menu, view / Edit geometry data, click File and Open Geometry Data, selecting the previously created geometry, following the procedure in diagram 2.

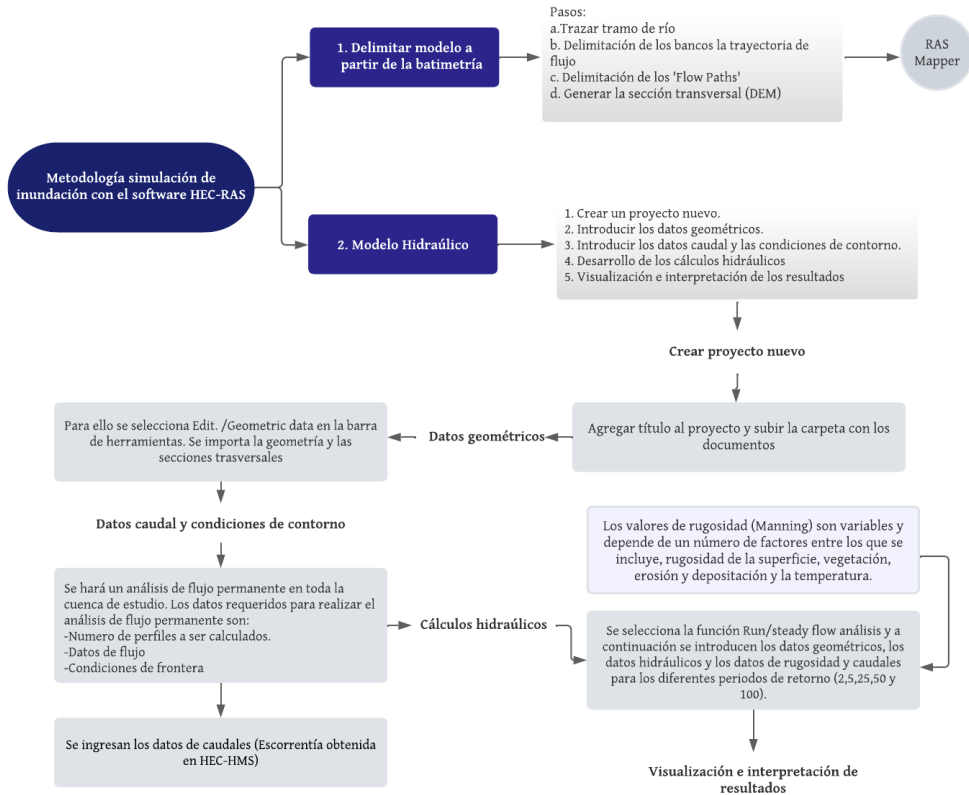


Diagram 2. Flood simulation for a stretch of the Teusacá River. Hec -Ras.

3. Results and Discussion

The Teusacá River sub-basin crosses eight municipalities: Bogotá, La Calera, Sopó, Tocancipá, Chía, Choachí, Ubaque, and Guasca[1]. However, although these municipalities are located within the same department, they are associated with different administrative entities, and their percentage distribution is very diverse. Some municipalities include both the municipal seat and part of the urban area within the basin, while others cover only the rural area. The Teusacá River sub-basin has an area of 362,445 km², according to Campos.[15] This parameter is directly related to discharge flow, since the size and location of the basin determines the captured precipitation, surface runoff, and water storage capacity. A larger basin means a larger drainage area, meaning there is more surface area to receive rainfall. Similarly, the larger the area, the greater the amount of water that becomes runoff. However, it is important to take into account the geographic area

where the basin is located, since it plays an important role in the runoff generated. According to the Campos classification [15], basins within the range of 250 to 500 km² are classified as Intermediate-Small, within which range the study basin is located (see Table 4), which corresponds to an area of rapid hydrological response since it presents shorter distances and shorter concentration times [16]. Its perimeter was 130.53 km; it runs along the watershed, indicating the limit of the basin, as does the average width, since this parameter indicates a relationship between the area and its average length. Regarding lengths, these measurements alone make it very difficult to infer an in-depth analysis; however, they are used to find other indices that are relevant when studying morphometry.

Following the above, the shape of the basin was analyzed using three corresponding indices (i) shape index, (ii) compactness index and (iii) elongation ratio that relate the area to the main channel. However, it is noted that these indices do not include the relief factor. The shape index (F) is a dimensionless parameter that indicates the way in which surface runoff is controlled, this factor will take values lower than 1 in the case of elongated basins, while when it approaches 1 or has a higher value, they are closer to a circular shape [17]. In this case, the value was 0.184, which, according to Horton's classification, the area is in the very elongated category; which coincides with the shape of the basin, see Figure 1. A basin with a low shape index is less likely to be affected by torrential rain events [18].

Table 4. Morphological parameters of the basin	
Morphological parameters	
Main channel length (km)	61,097
Basin area (km ²)	362,445
Perimeter of the basin (km)	130.53
Average length of the basin (m)	45.13
Average width of the basin (m)	8,031
Drainage density (km/km ²)	1,704
Form factor	0.184
Elongation ratio	0.484
Compactness index or Gravelius	1.8
Highest point masl	3,518.89
Lowest point masl	2,550
Average slope of the basin	10.77
Average slope of the main channel	0.0158
Concentration time (min)	463,356

Note: Values obtained by ArcGIS processing.

Graveliuscompactness index (Kc) relates the perimeter of the basin with that of a circle or equivalent area. Kc is associated with the concentration time, which expresses the time it takes for a raindrop to travel from the furthest part of the basin to the exit point. The closer the coefficient is to 1, the rounder the basin will be; in this case, the basin's susceptibility to flooding increases. This is because the distances between points on the watershed with respect to a central one are more uniform, resulting in shorter concentration times, generating continuous flood waves. However, when basins tend to be more elongated, as in this case, the probability of flooding is reduced [16]. In this case, the result was 1.8, classifying it as oval, oblong, or oblong-

rectangular. Basins with a high compactness coefficient may have shorter concentration times, since rainwater tends to converge more quickly towards the central point of the basin [19].

Finally, the elongation ratio (Re) relates the diameter of a circle with an area similar to that of the basin and the maximum length of the basin, explaining the relationship of the area with the main channel. This index is closely related to hydrology [18], according to González, [20] values less than 1 indicate basins that have an elongated shape and values close to or greater than 1, their shape tends to be round. For the basin studied, its value was 0.484, which again indicates its elongated shape. A basin with this type of shape will have a lower probability of experiencing intense and simultaneous rainfall that covers the entire surface, reflecting a lower magnitude in the floods as mentioned above.

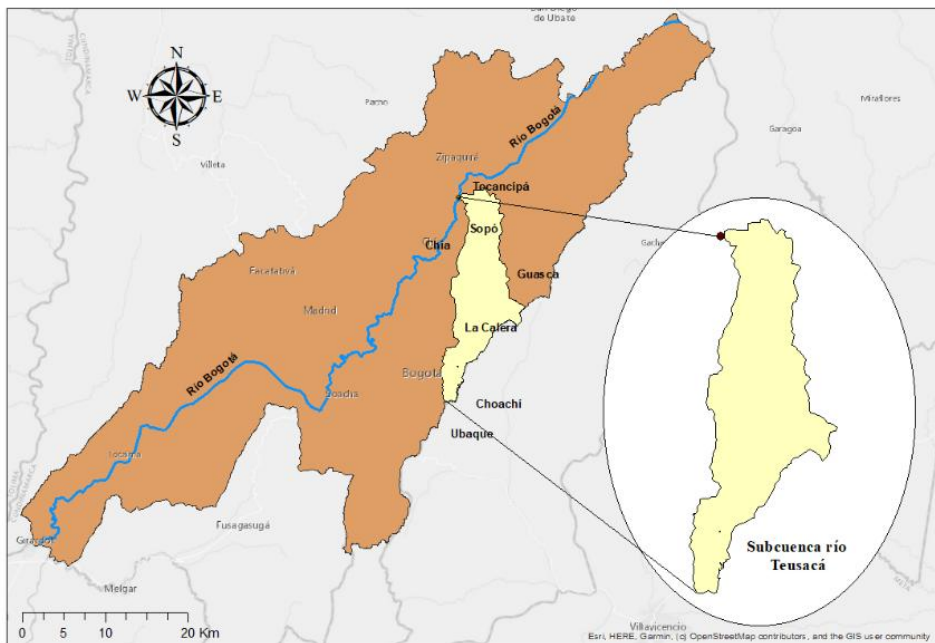


Figure 1. Location of the Teusacá River sub-basin.

The relief parameters provide third-dimensional information, including the maximum and minimum heights of the basin, the average slope of the main channel, and the average slope of the basin; the average slope of the main channel can reflect the channel's response capacity to the intensity of torrential rains, while the average slope of the basin can indicate the runoff velocity [18]. Basins with greater inclination tend to react more quickly to precipitation, experiencing an increase in flow [21]. Likewise, basins with a very steep slope are more susceptible to erosion, since the speed of the water is faster and there is greater kinetic energy, favoring soil wear [22]. According to the POMCA classification [1], basins that are within the 7

to 12% range are classified as moderately rugged, therefore, the inclination of the basin is moderate, showing a diverse topography between valleys and hills. Related to the previous analysis of rising water levels, when a basin has steep slopes, there is a tendency for floods to occur in short periods of time [1]. This classification can be seen in Figure 2, where most of the basin has an elevation percentage between 7 and 12%.

The hypsometric curve represents the variation in the average elevation of the basin, where the distribution of the different heights of the basin can be observed [23]. These elevation values are considered when studying temperature and precipitation. There is no universal classification to separate the basin into high, medium, and low. However, characteristics such as hypsometry and the longitudinal profile of the main channel can provide an analysis from a hydrographic perspective [24]. From Figure 2, we can see that the average elevation of the basin is 2,900 meters above sea level. According to the Strahler classification, the basin is classified as an old river.

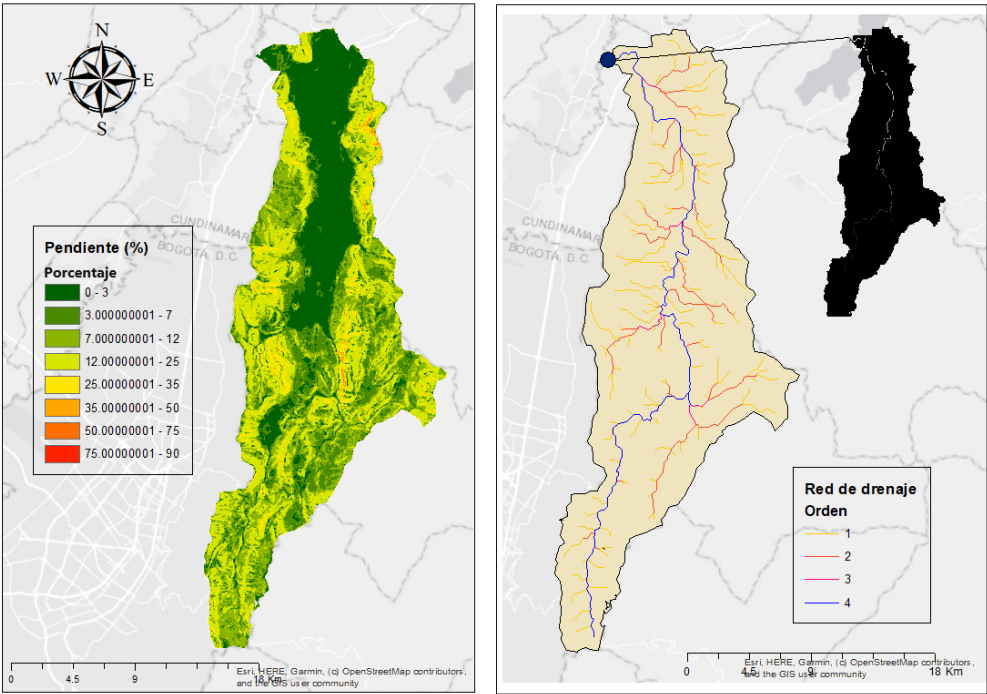


Figure 2. Slope and drainage order of the Teusacá River.

Teusacá River basin.

On the other hand, regarding vegetation cover, variations were evident between 2000 and 2018. Generally, changes in land cover are mostly caused by human activity aimed at manipulating the landscape and nature to meet their needs; this change in land cover may reflect the possible use

being given to the land. According to Pedraza, [4] in recent decades during the 20th century, there was an increase in deforestation and the conversion of forest areas into crop areas. In addition, Carrero, [2] who cites other authors, agrees that territorial occupation intensified, mainly in the upper-middle part of the basin, given the job offers provided by the owners of the haciendas and properties. The author also highlights that the most relevant changes occurred in the 1920s; by the end of the 1930s, livestock farming and deforestation activities were already evident. At the same time, the introduction of foreign species such as pines and eucalyptus, urban expansion, industrial growth, and the use of chemicals in agriculture increasingly dominated the basin. By the late 1960s, agriculture had become the most important economic activity. This demand continued to grow to meet the needs of the basin's inhabitants, and outside the basin, by the 2000s, little native forest remained due to the expansion of livestock production systems, focused primarily on raising cattle for milk production. This is consistent with the map presented in Figure 4, since, by 2000, forest cover represented 1.73% and crop cover 2.43%. The remaining percentage is divided between pastures, shrubs, secondary vegetation, mining and industrial extraction areas, urban fabric, and bare or degraded areas.

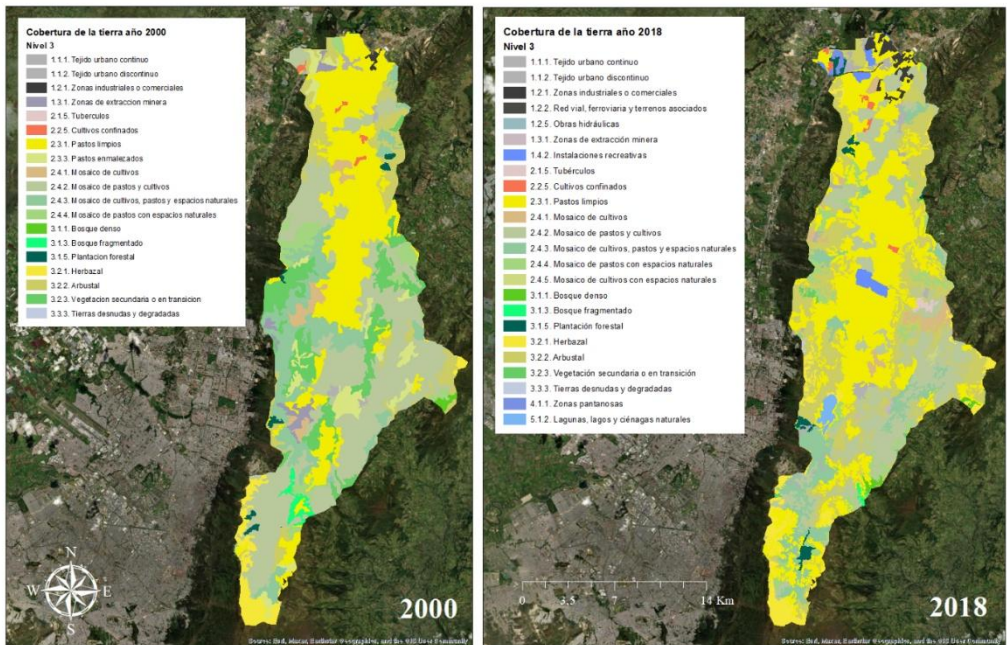


Figure 4. Vegetation cover in 2000 and 2018 based on CLC classification in the Teusacá River area.

Likewise, Figure 4 shows that by 2018, the area of crops, pastures, and natural spaces decreased, with clean pasture cover predominating, representing more than 35% of the study area, while forest cover accounted for 1.51% and crops 2.13%. This is consistent with the Teusacá River POMCA conducted by Planeación Ecológica Ltda et al. [1], where pasture cover overcasted

almost half of the basin. This cover is related to land use; in this case, it is intended for grazing and raising dairy cattle, which is distributed from north to south in its central part, becoming the most important activity in the area, mainly in the municipality of La Calera. However, it presents a land use conflict given these agricultural activities and urbanization projects in areas designated for cultivation in protected areas. This conflict becomes a direct cause of soil degradation and contamination of natural resources [25]. This degradation is linked to the effects of deforestation in conservation areas, changes in land use and habitat transformation, which generate environmental problems such as loss of vegetation cover, alteration of ecological services, increase in pollutant loads, etc.[26].

Similarly, according to Blanco & Martínez, [24]over the years, there has been an increase in the urban fabric due to significant growth in the construction sector. In 2011, especially in the municipality of Sopó, the growth rate was reported to have reached 79.1%, resulting in an increase in the number of buildings constructed compared to previous periods. As reflected in Figure 4, in 2000, the urban fabric represented 0.71% of the basin, while in 2018 it represented 1.91%.

Vegetation cover dynamics and land use are important characteristics for estimating the curve number (CN), in addition to the soil hydrological group (GH) and terrain slope. This hydrological parameter represents the soil's infiltration capacity and its response to precipitation, relating to the amount of water flowing through the basin [11]. Given the size of the basin studied, it was divided into 19 micro-basins, and the average CN was calculated for each of them, thus creating Table 5.

Table 5. Curve number results for 2000 and 2018.

Micro-basin	CN Prom 2000	CN Prom 2018
1	81,623	80,463
2	81,587	81,046
3	79,873	79,720
4	82,551	82,751
5	80,277	79,648
6	80,281	79,622
7	81,333	81,482
8	81,458	81,366
9	80,528	80,928
10	81,725	81,272
11	82,111	82,701
12	82,857	82,711
13	82,138	83,713
14	82,287	80,574
15	81,481	81,520
16	81,732	84,378
17	84,951	84,551
18	83,229	83,989
19	82,990	82,582

Note: Values extracted from ArcGis ; CN: Curve number.

As can be seen, the values do not experience abrupt changes, but rather minimal ones. The weighted average curve number for the studied basin had a value of 81.8 for both years, indicating that the conditions of the territory favor runoff rather than infiltration. Values close to zero indicate very high permeability, while values close to 100 indicate impermeability [28].

This finding is consistent with studies conducted by Carvajal & Fernández [29] and Gualdrón et al. [30], who also determined the curve number in the Betancí sub-basin (Córdoba, Colombia) and the upper Suárez River basin (Saboya, Colombia), respectively. In this case, both basins had similar characteristics to the analyzed sub-basin, especially with regard to vegetation cover, since most of their area was occupied by pastures used for extensive livestock farming. The average CN value in one of the studies was 83; the other, although the average was not mentioned, showed a range of 80 to 100, indicating a high capacity to generate runoff, according to the classification given by the curve method. This runoff potential makes the basin susceptible to water erosion if it has bare areas, since a large amount of water, by not infiltrating, flows over the surface, increasing the amount and speed at which it moves through the basin, dragging soil particles, sediments and organic materials along the soil surface. The magnitude of the erosion will depend on the slopes [31].

Although crops predominated in 2000 compared to 2018, the CN value was very similar to that of 2018. This is because, despite differences in vegetation, soil characteristics play a relevant role in estimating the value. In both years, the hydrological groups were the same, and when combined with vegetation cover, they resulted in similar values. Furthermore, variations in the curve number in each of the microbasins are due to the spatial distribution of soil cover and hydrological groups. These factors contribute significantly to the differences observed in CN values between different areas of the basin.

As an example, the study carried out by Tailor & Narendra, in the [11]Mehsana district basin, India, revealed an average value of 76 for the bend number. It is important to highlight that this basin is mainly characterized by the presence of crops, which could suggest a lower propensity to runoff. However, despite this predominant vegetation cover, the value obtained was considerably high. This result underlines the significant influence of geographical conditions on the estimation of the bend number, highlighting the complexity and importance of taking all factors into account when analyzing this hydrological parameter.

To understand the hydrological behavior of the basin, the average monthly maximum precipitation was considered, which plays a crucial role in runoff and flood potential. The precipitation recorded by the hydrometeorological stations of San Luis 1 and San Luis 2, La Casita, San Pedro, and Parque Sopo was also taken into account. Using the values derived from the IDF curves in equation 8, the precipitation intensities corresponding to different durations and frequencies of occurrence were calculated for the return periods of 2, 5, 25, 50, and 100 years, as projected in Table 6.

Table 6. Alternating precipitation.

Minute	Alternating Precipitation (mm)				
	T=2	T=5	T=25	T=50	T=100
5	0.209	0.241	0.309	0.344	0.382
10	0.217	0.250	0.320	0.356	0.396

15	0.226	0.260	0.333	0.371	0.412
20	0.236	0.271	0.347	0.386	0.430
25	0.246	0.284	0.363	0.404	0.450
30	0.259	0.298	0.381	0.424	0.472
35	0.273	0.314	0.402	0.447	0.497
40	0.289	0.332	0.426	0.474	0.527
45	0.308	0.354	0.453	0.504	0.561
50	0.330	0.380	0.487	0.541	0.602
55	0.357	0.412	0.527	0.586	0.652
60	0.392	0.451	0.578	0.642	0.715
65	0.436	0.502	0.643	0.715	0.796
70	0.497	0.572	0.733	0.815	0.907
75	0.587	0.675	0.865	0.962	1,070
80	0.737	0.848	1,086	1,208	1,344
85	1,063	1,224	1,568	1,744	1,940
90	4,843	5,575	7,140	7,942	8,835
95	1,475	1,698	2,175	2,419	2,691
100	0.861	0.991	1,270	1,412	1,571
105	0.651	0.749	0.959	1,067	1,187
110	0.537	0.618	0.792	0.881	0.980
115	0.464	0.534	0.684	0.761	0.847
120	0.412	0.475	0.608	0.676	0.752
125	0.374	0.430	0.551	0.613	0.682
130	0.343	0.395	0.506	0.563	0.626
135	0.318	0.366	0.469	0.522	0.581
140	0.298	0.343	0.439	0.488	0.543
145	0.280	0.323	0.413	0.460	0.512
150	0.265	0.306	0.391	0.435	0.484
155	0.252	0.291	0.372	0.414	0.460
160	0.241	0.277	0.355	0.395	0.439
165	0.231	0.266	0.340	0.378	0.421
170	0.222	0.255	0.327	0.363	0.404
175	0.213	0.246	0.314	0.350	0.389
180	0.206	0.237	0.303	0.338	0.375

Note: Values for constructing hyetographs from IDF curves. Station averages.

Hyetographs are graphical representations that show the temporal distribution of precipitation intensity during a rainfall event, allowing the analysis of rainfall behavior over a given period of time and its impact on runoff [32]. Table 6 shows a direct relationship between the increase in the return period and the intensification of precipitation. This phenomenon is explained by the nature of the return period, which represents the expected time between successive occurrences of an event of a certain magnitude [33]. In this case, the maximum monthly precipitation event is used as a reference. This parameter is also related to the concept of climate change, according to the report of the Intergovernmental Panel on Climate Change (IPCC). Climate [31] highlights that climate change is increasing the frequency and intensity of extreme weather events, such as precipitation and heat waves. Furthermore, studies such as that by Hirsch & Ryberg [32] they have found a global trend toward greater variability in precipitation patterns, which can result in

changes in the frequency and magnitude of extreme events. This indicates that events that previously occurred rarely, such as intense storms, are now occurring with greater frequency and intensity.

On the other hand, in the context of HEC-HMS modeling, it is essential to consider flow routing, for which different methods exist. For this purpose, the Muskingum method was used, which plays a crucial role in predicting flow propagation along the channel. This prediction takes into account both the geomorphological characteristics and the storage capacity of the channel [36]. In the Muskingum method, variables k and x are related to flow routing along a channel or river, where k is a constant called the storage parameter and x is a weighting factor that expresses the relative influence of storage inputs and outputs in the reach. These variables are used to determine the speed and direction in which a flow wave will propagate along the channel [37]. According to equation 9 and equation 10, the values of the variable k were determined. For the variable x , a value of 0.2 was selected, which is a recommended average value according to the literature on flow circulation [36]. The results of the calculation of the variable k can be seen in Table 7.

Table 7. k and x values. Muskingum method.

Stretch	k	x
1	2,229	0.2
2	2,455	0.2
3	4,791	0.2
4	0.952	0.2
5	2,876	0.2
6	2,214	0.2
7	0.855	0.2
8	0.288	0.2
9	0.570	0.2

Note: Values entered into the hec-hms program.

Finally, when the program is run, the corresponding flows are generated for each microbasin, section, junction, and sink. In this case, the flows leaving the basin, that is, those from the sink, are taken into account during the different return periods and years, for both 2000 and 2018, as shown in Table 8.

Table 8. Flow rates obtained from the HEC-HMS program.

Year	Maximum flow rate m^3/s				
	Return period (years)				
	2	5	25	50	100
2000	8.5	14.4	31.3	41.9	55
2018	9.4	15.5	32.9	43.7	57

Note: Maximum flows according to return period for the Teusacá River basin.

According to the Hydrographic Basin Management and Planning Plan (POMCA), the average flow generated in the basin ranges between 6 and 10 m^3/s per year, while the flows for the different return periods vary between 25.6 and 65.9 m^3/s [1]. These values were taken from the

analysis developed in the "Environmental Impact Study for the Construction of San Rafael Park." However, the methodology used to obtain these results is not clearly explained by the author.

On the other hand, an increase in flow rates is observed for 2018 when adjusting the curve number values for that year. Although the variation in the curve number values was minimal, an increase in flow rates of between 1 and 2 m³/s was achieved compared to 2000, highlighting the relationship between coverage and the hydrological regime. This phenomenon is also reflected in the study conducted by Crespo et al. [35], where they studied land-use change on hydrology in the humid páramos of southern Ecuador, using paired micro-basins. The authors observed that the outflow from the micro-basin with crops is lower than that of the micro-basin with intensive grazing cover, recording values of 32.9 l/s/km² and 20.5 l/s/km², respectively. They also mention that the cultivated microbasin shows a decrease in low and medium flows and an increase in peak flows, suggesting a considerable loss of water regulation capacity, attributed to various factors such as increased hydraulic conductivity, the construction of artificial drainage systems, and soil compaction. They also point out that when animal density is low and rotation techniques are used, the hydrological response is not significantly affected.

Similarly, Gelvez[36]iIn a similar study in the Coello River basin, he mentions changes in land use in recent years, such as increased urbanization and, consequently, in agricultural and livestock activities, the latter being the most predominant. These changes have resulted in a reduction in natural vegetation cover, such as forests, favoring lower vegetation. The author notes that, after conducting various simulations, an increase in monthly flow values was observed, from 21.93 m³/s to 54.29 m³/s. This increase is attributed to the decrease in evapotranspiration due to cover transitions, where the lower presence of forest cover reduces the evaporative effect of plant leaves. Furthermore, tree roots have a greater capacity to extract moisture from the soil compared to areas with lower vegetation, which reduces retention capacity and leads to an increase in long-term discharge into the main waterways of the basin [40].

While vegetation is related to water storage, a tropical rainforest has the capacity to store large amounts of water, grass roots can barely extract water below 50 cm, while tree roots reach several meters. In addition, trees can store up to 12% of precipitation in their leaves and other depressions [41]. Similarly, authors Lee et al. [42]and Moraes et al. [43]agree that changes in soil cover alter evapotranspiration, soil moisture content, groundwater recharge, runoff processes, and river flow. They emphasized that the replacement of deep roots with grasses or shallower roots increases soil moisture, groundwater recharge, infiltration and storage capacity, etc. Therefore, the shift in economic activity from agriculture to livestock activities in the Teusacá River basin has resulted in an increase in the outflow from said basin.

It is worth highlighting that these hydrological models are usually complex given the number of variables that play an important role, such as climate change, which has a direct influence on runoff, which is one of the main components of the hydrological cycle [44]. According to Lin et al. [45], the influence of climate variability is more significant on surface hydrology than land use change, however, accurately determining the impact of temperature change is complicated, since thermal fluctuations also exert their own influence on other hydrometeorological variables.

Likewise, considering the complexity of hydrological models and the influence of climate change, it is crucial to understand how flow levels can influence flood probability. Changes in precipitation patterns and temperature can significantly affect the magnitude and frequency of runoff events, which in turn can increase flood risk in certain areas. Figure 5 visualizes the area chosen to assess flood zones.

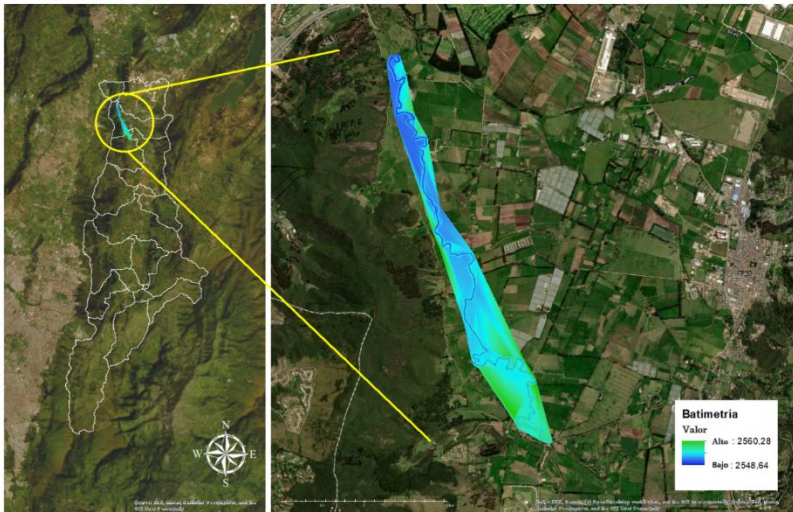


Figure 5. Bathymetry of the area susceptible to flooding in the Teusacá River basin.

The stretch of the river where flood susceptibility was assessed is located in the municipality of Sopó, as it is most susceptible due to its geomorphological conditions. According to the Hydrographic Basin Management and Planning Plan (POMCA) [1], areas with slopes less than 3% are considered at risk of flooding. Figure 2 shows that the municipality of Sopó has slopes ranging from 0 to 3%, making it susceptible to flooding. In 2008, the Regional Autonomous Corporation of Cundinamarca (CAR) issued an alert to residents near the Teusacá River in the Sopó Valley and in the municipalities of the middle Bogotá River basin, due to the risk of flooding caused by the intense and persistent rains that fell that same year [46]. Likewise, given the presence of heavy rains caused by the La Niña phenomenon in 2011, mainly in the Colombian Andes, the Bogotá savanna reached its maximum water storage capacity, affecting several municipalities in Cundinamarca. As a result of these conditions, 95% of the department of Cundinamarca was affected and more than 30,000 hectares were flooded due to heavy rains, a phenomenon that was repeated in 2020 and 2011 [46]. According to the flows obtained in the HEC-HMS model (Table 8), areas susceptible to flooding have been identified after a 5-year return period.

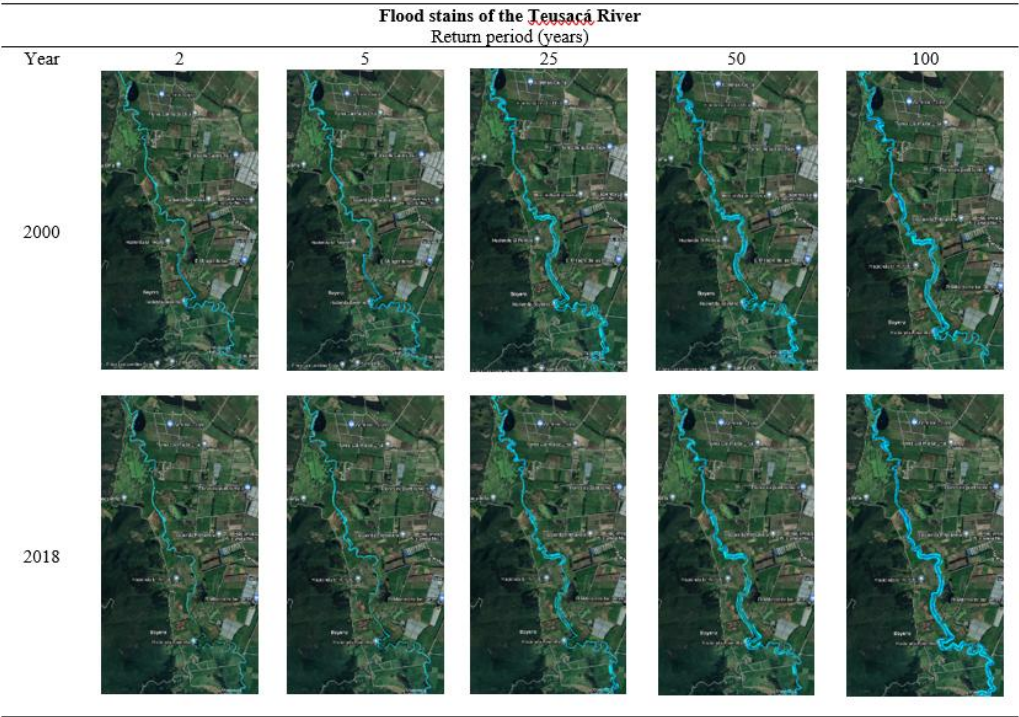


Figure 6. Flood patches in the different return periods

Through the images presented in Figure 6, it can be seen that the areas most prone to flooding in 2000 were located mainly in the upper and middle sections of the river stretch, with water levels ranging between 0.5 and 2 meters. On the other hand, by 2018, it is observed that the most vulnerable areas are both the upper and lower sections of the river stretch, with water levels varying between 0.7 and 2.3 meters. This analysis suggests that, as the return period increases, flood depth tends to increase in certain areas. It is also worth noting that the modeled stretch of the Teusacá River is characterized by low slopes, which causes the flow in the channel to be predominantly subcritical, presenting high flow depths and low velocities [47]. This highlights the importance of considering this factor when assessing flood risk and planning appropriate mitigation measures. Figure 7 shows one of the cross sections located in the upper reaches of the river, which shows flooding for the 25-, 50-, and 100-year return periods, since the power line overflows the riverbank during these periods. However, although there are areas that do not experience flooding, the purpose of channel improvements is to carry out a comprehensive restoration, maintaining uniform widths and widening sections, especially where tributaries enter.

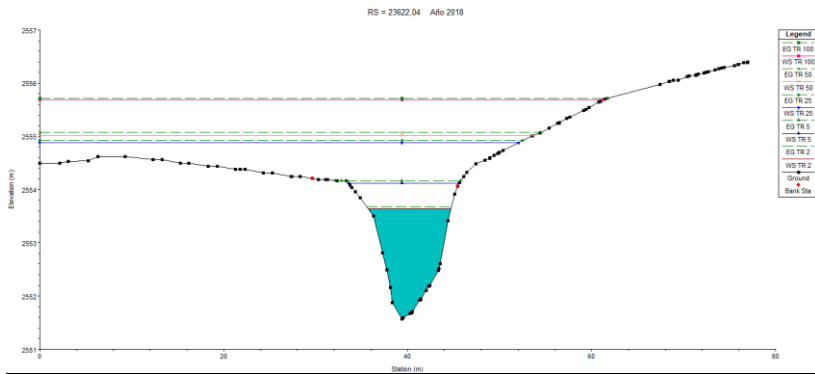


Figure 7. Cross section of the upper part of the Teusacá River stretch.

In this regard, when making channel improvements, it is essential to thoroughly assess the retention capacity and design measures that allow for optimal water flow regulation, taking into account hydrological conditions and the needs of the local community. According to the modeling, for the year 2000, the water volume reached 350 m³, while for the year 2018, the volume during these same return periods was 300 and 500 m³, respectively (Figures 8 and 9).

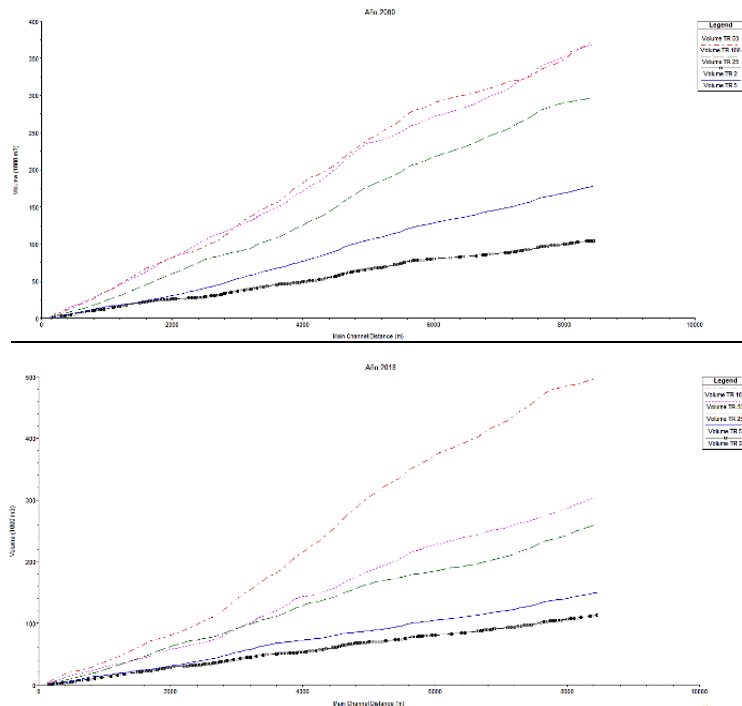


Figure 8 and 9. Volume vs. Channel Distance

4. Conclusions

Soil hydrologic conditions are influenced by a variety of factors, including soil characteristics and vegetation cover, whose complex interactions determine the soil's capacity to retain and release water. Likewise, the rate of change in the hydrologic response to land-use change is influenced by the intensity of the change or transition from natural vegetation to another type of cover through human activity and the location within the watershed. Adjusting the curve number values for 2018 led to a significant increase in streamflow. This finding is consistent with previous research that has shown how land-use change, particularly toward agricultural activities, can affect a region's hydrology, increasing streamflow and decreasing water regulation capacity. Similarly, decreased forest cover and the expansion of low vegetation contribute to this phenomenon by reducing evapotranspiration and soil retention capacity.

It is important to mention that the quality of the available hydrometeorological time series can be a significant challenge in hydrological research, as they contain numerous gaps, in addition to high variability and hydrometeorological gradients, making it difficult to accurately characterize the hydrological response. Despite this, satisfactory results were achieved, demonstrating that there is indeed a relationship between vegetation cover and the river's hydrological regime.

On the other hand, the analysis carried out on the stretch of the river located in the municipality of Sopó highlights the importance of considering flood susceptibility in areas with slopes less than 3%, as indicated in the Hydrographic Basin Management and Planning Plan (POMCA). The presence of slopes within this range in the municipality of Sopó makes it particularly vulnerable to flooding events. However, despite the change in coverage, overflow phenomena occur in both scenarios. It is noteworthy that, by 2018, the water table in some locations was higher than in 2000. This modeling highlights the need to implement risk management measures in the area, especially in the face of relatively short-term events such as the 5-year period, to mitigate the potential impacts of flooding on the local population and infrastructure.

WORKS CITED

- [1] Planeación Ecológica Ltda, Ecoforest Ltda, Elaboración del Diagnóstico, Prospectiva y Formulación de la Cuenca Hidrográfica del río Bogotá Subcuenca del río Teusacá - 2120-13, 2013. <https://www.car.gov.co/uploads/files/5ac25d4c03bce.pdf>
- [2] L. Carrero, reconstrucción histórica e interpretación de los procesos de transformación en el uso y manejo del paisaje en la cuenca alta del río Teusacá. Bogotá, Cundinamarca, (2012). <https://repository.javeriana.edu.co/handle/10554/12459>.
- [3] C. La verde, Servicios ecosistémicos que provee el páramo de la cuenca alta del río Teusacá: Percepción de los actores campesinos y su relación con los planes ambientales en la vereda Verjón Alto, Bogotá D.C., Bogotá D.C, 2008.
- [4] L. Pedraza, análisis y evaluación del impacto ambiental de los procesos de urbanización en el sector de la cuenca media-baja del río Teusacá, municipios de la Calera, Guasca y Sopó, Bogotá, D.C, 2014. <https://repository.javeriana.edu.co/handle/10554/15007>

- [5] F. Nardi, A. Annis, C. Biscarini, On the impact of urbanization on flood hydrology of small ungauged basins: the case study of the Tiber River tributary network within the city of Roma, *Flood Risk Management* Volume 11 (2018).
<https://doi.org/https://doi.org/10.1111/jfr3.12186> (accessed March 4, 2024).
- [6] S.L. Muñoz, D.C. Beltrán, perfil ambiental de la subcuenca del río Teusacá de la cuenca alta del río Bogotá, Bogotá D.C., 2010.
https://ciencia.lasalle.edu.co/cgi/viewcontent.cgi?article=1038&context=ing_ambiental_sanitaria.
- [7] E.A. Maldonado, Estimación de caudales medios para la subcuenca del río Teusacá mediante el software hec-hms, Bogotá D.C., 2018.
- [8] P. Serrano-Muela, E. Nadal-Romero, N. Lana-Renault, La relación suelo-vegetación y su influencia en el comportamiento hidrológico de distintos ambientes vegetales, Zaragoza, 2014. <https://dialnet.unirioja.es/descarga/articulo/4854048.pdf>
- [9] J. Prieto Villarroya, H.D. Farias, M.E. Amarilla, Estimación del parámetro hidrológico del Número de Curva NC: Automatización del cálculo mediante S.I.G. y nuevas fuentes de información cartográfica. Caso del área urbana de Pozo Hondo, 2013.
<https://fcf.unse.edu.ar/archivos/publicaciones/codino-a-2013/trabajos/tierra/27-prieto.pdf>.
- [10] S. Ibáñez, H. Moreno, J. Gisbert, Valores del no de curva (cálculo de la escorrentía), 2021.
<https://riunet.upv.es/bitstream/handle/10251/10783/Valores%20del%20n%C2%BA%20de%20curva.pdf>
- [11] D. Tailor, J. Narendra, Surface runoff estimation by scs curve number method using gis for rupan-khan watershed, Mehsana district, Gujarat, 36 (2016).
- [12] H.K. Shukur, Estimation Curve Numbers using GIS and Hec-GeoHMS Model, 2017.
- [13] G. Villamizar, Y. Calderón, Proyecto Compilación y Levantamiento de la información Geomécánica. Desarrollo Cartografía Edáfica Aplicado a la Ingeniería en la Sabana de Bogotá, 2005.
- [14] M. Tewolde, J. Smithers, Flood routing in ungauged catchments using Muskingum methods, 32 (2006). <http://www.wrc.org.za>.
- [15] D. Campos Aranda, Procesos del ciclo hidrológico, 1998.
<https://repositorio.institucional.uaslp.mx/xmlui/handle/i/3331>
- [16] M. Vásquez, A. Mancheno, C. Álvarez, C. Preh, C. Cevallos, L. Ortiz, Cuencas Hidrográficas, 2019.
- [17] M. Jardí, Forma de una cuenca de drenaje. Análisis de las variables morfométricas que nos la definen, (1985) 41-68.
<https://www.raco.cat/index.php/RevistaGeografia/article/download/45789/56812/0>
- [18] M.A. Camino, J. Bó, J. Cionchi, J. Del Rio, A. López de Armentia, S. De Marco, Estudio morfométrico de las cuencas de drenaje de la vertiente sur del sudeste de la provincia de Buenos Aires, 27 (2018).
- [19] S. Mohammad, T. Fakhrabadi, J. Chezgi, Effect of morphometric factors in prioritizing flooding of sub-watersheds in the north of Birjand Plain, (2022).
<https://doi.org/10.22098/mmws.2022.11855.1179>.
- [20] A.I. González De Matacoa, Análisis morfométrico de la cuenca y de la red de drenaje del río Zadorra y sus afluentes aplicados a la peligrosidad de crecidas, 2004.
<https://dialnet.unirioja.es/descarga/articulo/1079160.pdf>
- [21] R.E. Horton, Erosional development of streams and their drainage basins; Hydrophysical approach to quantitative morphology, *Bulletin of the Geological Society of*

- America 56 (1945) 275-370. [https://doi.org/10.1130/0016-7606\(1945\)56\[275:EDOSAT\]2.0.CO;2](https://doi.org/10.1130/0016-7606(1945)56[275:EDOSAT]2.0.CO;2).
- [22] C. Camargo, C. Pacheco, R. López, Erosión hídrica, fundamentos, evaluación y representación cartográfica: una revisión con énfasis en el uso de sensores remotos y Sistemas de Información Geográfica, Gestión y Ambiente 20 (2017) 265-280. https://doi.org/10.15446/ga.v20n2.____.
- [23] J.M.G. Racca, J. Manuel, G. Racca, Análisis hipsométrico, frecuencia altimétrica y pendientes medias a partir de modelos digitales del terreno, 2007. <http://www.fceia.unr.edu.ar/fisiografia/publicaciones.htm>. Recibido: 01/06/2007
- [24] F. Guerra, J. González, Caracterización morfométrica de la cuenca de la quebrada La Bermeja, San Cristóbal, Estado Táchira, Venezuela, 7 (2002) 88-108. <http://www.redalyc.org/articulo.oa?id=36070208>.
- [25] A. Salinas, D. González, Propuesta ambiental para el plan de desarrollo del municipio de la calera, Cundinamarca para el período 2020- 2024., Bogotá D.C, 2019.
- [26] G. Andrade, L. Castro, Degradación, pérdida y transformación de la biodiversidad continental en Colombia Invitación a una interpretación socioecológica, (2012). <https://dialnet.unirioja.es/descarga/articulo/4021796.pdf>
- [27] I. Blanco, N. Martínez, Análisis multitemporal de la calidad del agua en relación con la cobertura de la tierra en la subcuenca media y baja del río Teusacá, 2023.
- [28] D.E. Woodward, R.H. Hawkins, R. Jiang, A.T. Hjelmfelt, J.A. Van Mullem, Q.D. Quan, Runoff curve number method: Examination of the initial abstraction ratio, in: World Water and Environmental Resources Congress, American Society of Civil Engineers (ASCE), 2003: pp. 691-700. [https://doi.org/10.1061/40685\(2003\)308](https://doi.org/10.1061/40685(2003)308).
- [29] Á.D. Carvajal, T. Fernández, Determinación del número de curva en la subcuenca de Betancí (Córdoba, Colombia) mediante teledetección y SIG, Ingeniería y Desarrollo 32 (2017) 200-217. <https://doi.org/10.14482/inde.32.2.5406>.
- [30] D.F. Gualdrón, J.J. Villate, A.P. Rodríguez, Cálculo y aplicación del método del número de curva del soil conservation services (scs) para la cuenca alta del río Suárez usando sistemas de información geográfica, 2021.
- [31] R.P.C. Morgan, J.N. Quinton, R.E. Smith, G. Govers, J.W.A. Poesen, G. Chisci, D. Torri, The european soil erosion model (eurosem): a dynamic approach for predicting sediment transport from fields and small catchments, in: Modelling Soil Erosion by Water, Springer Berlin Heidelberg, 1998: pp. 389-398. https://doi.org/10.1007/978-3-642-58913-3_29.
- [32] K. Wartalska, B. Kaźmierczak, M. Nowakowska, A. Kotowski, Analysis of hyetographs for drainage system modeling, Water (Switzerland) 12 (2020). <https://doi.org/10.3390/w12010149>.
- [33] A. Bateman, Hidrología básica y aplicada, 2007.
- [34] Intergovernmental Panel on Climate Change, Land-climate interactions, in: Climate Change and Land, Cambridge University Press, 2019: pp. 131-248. <https://doi.org/10.1017/9781009157988.004>.
- [35] R.M. Hirsch, K.R. Ryberg, Has the magnitude of floods across the USA changed with global CO₂ levels?, Hydrological Sciences Journal 57 (2012) 1-9. <https://doi.org/10.1080/02626667.2011.621895>.
- [36] J. Luis. Ayuso, Circulación de flujos: Métodos de cálculo usuales en el diseño de canales y embalses en cuencas pequeñas, Universidad de Córdoba, 1990.
- [37] F. Javier. Aparicio, Fundamentos de hidrología de superficie, Noriega, 1989.

- [38] P. Crespo, R. Célleri, W. Buytaert, B. Ochoa, I. Cárdenas, V. Iñiguez, P. Borja, B. De Bièvre, Impactos del cambio de uso de la tierra sobre la hidrología de los páramoshúmedosandinos, 2014.
- [39] J. Gelvez, Efectos del cambio en el uso y cobertura del suelo sobre el régimen hidrológico de la cuenca del río Coello, 2021.
- [40] M. Peraza, E. Ruiz, M. Meaurio, S. Sauvage, J.M. Sánchez, Modelling the impact of climate and land cover change on hydrology and water quality in a forest watershed in the Basque Country (Northern Spain), *EcolEng* 122 (2018) 315-326. <https://doi.org/10.1016/j.ecoleng.2018.07.016>.
- [41] G. Poveda, O.J. Mesa, Efectos hidrológicos de la deforestación, 2016.
- [42] E. Lee, A. Livino, S.C. Han, K. Zhang, J. Briscoe, J. Kelman, P. Moorcroft, Land cover change explains the increasing discharge of the Paraná River, *Reg Environ Change* 18 (2018) 1871-1881. <https://doi.org/10.1007/s10113-018-1321-y>.
- [43] J.M. de Moraes, A.E. Schuler, T. Dunne, R. de O. Figueiredo, R.L. Victoria, Water storage and runoff processes in plinthic soils under forest and pasture in Eastern Amazonia, *Hydrol Process* 20 (2006) 2509-2526. <https://doi.org/10.1002/hyp.6213>.
- [44] G.S. Dwarakish, B.P. Ganasri, Impact of land use change on hydrological systems: A review of current modeling approaches, *Cogent Geosci* 1 (2015) 1115691. <https://doi.org/10.1080/23312041.2015.1115691>.
- [45] Y.P. Lin, P.J. Wu, N.M. Hong, The effects of changing the resolution of land-use modeling on simulations of land-use patterns and hydrology for a watershed land-use planning assessment in Wu-Tu, Taiwan, *Landsc Urban Plan* 87 (2008) 54-66. <https://doi.org/10.1016/j.landurbplan.2008.04.006>.
- [46] W. Camargo, Implementación de modelación hidráulica con fines de pronóstico hidrológico, 2016.
- [47] Corporación Autónoma Regional, Informe Técnico No. 60195100073 - Corporación Autónoma Regional de Cundinamarca - CAR, 2019.